INFECTION AND IMMUNITY, Apr. 2008, p. 1476–1484 Vol. 76, No. 4
0019-9567/08/$08.00+0 doi:10.1128/IAI.01286-07
Copyright © 2008, American Society for Microbiology. All Rights Reserved.

Attenuated Endocytosis and Toxicity of a Mutant Cholera Toxin with Decreased Ability To Cluster Ganglioside GM_1 Molecules[▽]

Anne A. Wolf,[1] Michael G. Jobling,[2] David E. Saslowsky,[1] Eli Kern,[1] Kimberly R. Drake,[4] Anne K. Kenworthy,[4] Randall K. Holmes,[2] and Wayne I. Lencer[1,3]*

GI Cell Biology, Department of Pediatrics, Children's Hospital and Harvard Medical School,[1] and Harvard Digestive Diseases Center,[3] Boston, Massachusetts 02115; Department of Microbiology, University of Colorado Denver School of Medicine, Aurora, Colorado 80045[2]; and Departments of Molecular Physiology and Biophysics and Cell and Developmental Biology, Vanderbilt University School of Medicine, Nashville, Tennessee 37232[4]

Received 20 September 2007/Returned for modification 6 November 2007/Accepted 9 January 2008

Cholera toxin (CT) moves from the plasma membrane (PM) of host cells to the endoplasmic reticulum (ER) by binding to the lipid raft ganglioside GM_1. The homopentomeric B-subunit of the toxin can bind up to five GM_1 molecules at once. Here, we examined the role of polyvalent binding of GM_1 in CT action by producing chimeric CTs that had B-subunits with only one or two normal binding pockets for GM_1. The chimeric toxins had attenuated affinity for binding to host cell PM, as expected. Nevertheless, like wild-type (wt) CT, the CT chimeras induced toxicity, fractionated with detergent-resistant membranes extracted from toxin-treated cells, displayed restricted diffusion in the plane of the PM in intact cells, and remained bound to GM_1 when they were immunoprecipitated. Thus, binding normally to two or perhaps only one GM_1 molecule is sufficient for association with lipid rafts in the PM and toxin action. The chimeric toxins, however, were much less potent than wt toxin, and they entered the cell by endocytosis more slowly, suggesting that clustering of GM_1 molecules by the B-subunit enhances the efficiency of toxin uptake and perhaps also trafficking to the ER.

Cholera toxin (CT) causes the massive secretory diarrhea seen in *Vibrio cholerae* infections by hijacking an endogenous lipid-dependent trafficking pathway to enter the endoplasmic reticulum (ER) of host intestinal epithelial cells (18). CT is a two-component AB_5 toxin composed of an enzymatic A-subunit and a homopentameric B-subunit (32). The B-subunit can bind simultaneously to five ganglioside GM_1 molecules in the host cell plasma membrane (PM), and the B-subunit–GM_1 complex is the vehicle that carries the A-subunit from the PM to the ER (8). The A-subunit does not contribute to trafficking in this pathway. Once the A-subunit is in the ER, a portion of the A-subunit, the enzymatically active A1 fragment, dissociates from the rest of the toxin and retrotranslocates to the cytosol, where it activates adenylate cyclase to cause disease. In human intestinal T84 cells, this causes a cyclic AMP (cAMP)-dependent Cl^- secretory response (Isc) that can be measured in real time by electrophysiology. Other gangliosides and nonceramide lipids do not efficiently transport CT or CT-like toxins retrogradely into the ER, as assessed using human intestinal T84, green monkey kidney Vero, or rat glioma C6 cells (8, 22, 36). How GM_1 confers such specificity in lipid trafficking remains unexplained.

One hypothesis is that GM_1 associates the toxin with lipid rafts that function as platforms for trafficking CT through all or part of the retrograde pathway. Lipid rafts are thought to be small, highly dynamic membrane microdomains originating from self-assembly of cholesterol, sphingomyelin, glycolipids, and certain proteins that prefer a lipid-ordered microenvironment (4). Because lipid rafts are predicted to be small and very short lived (14, 19, 28), some functions attributed to them likely require a protein or protein scaffolding to stabilize the lipid microdomain or to coalescence a number of lipid rafts into larger structures that then have physiologic significance (2, 9, 19, 33). The CT B-subunit might provide such a protein scaffolding by binding five GM1 molecules and cross-linking them to stabilize or induce lipid raft function in toxin trafficking.

A previous study showed that chemically modified CT B-subunits with reduced numbers of binding sites are less toxic (6), but why this occurs remains unexplained. In this study, we tested whether clustering of GM_1 by the CT B-subunit affects toxin trafficking and thus function. To do this, we prepared a mixture of recombinant CT with B-subunits containing one, two, or no wild-type (wt) binding sites for GM_1. Because these toxins were prepared by genetic methods, the GM_1 binding sites were completely defined and were either identical to wt sites or completely inactive.

MATERIALS AND METHODS

Materials, cell culture and electrophysiology, and binding assays. Hanks' balanced salt solution (HBSS) (Sigma) supplemented with 10 mM HEPES (pH 7.4) was used for all assays unless indicated otherwise. Recombinant CT-H57A holotoxin was prepared as described previously (24). Antibodies directed to the CT B-subunit and the CT A-subunit have been described previously (17). wt CT was obtained from Calbiochem (San Diego, CA). All other reagents were obtained from Sigma Chemical Co. (St. Louis, MO) unless indicated otherwise. Cell culture and electrophysiology analysis were done as previously described (16, 17). Steady-state binding of wt CT and mutant toxins to T84 cells and inhibition of this toxin binding were measured exactly as described previously (24, 36).

Preparation of recombinant mutant holotoxins (CTB-G33D, CTB-W88K, and CT W88K/G33D). Plasmids pLMP148 and pLMP133 expressing G33D and W88K variants of the CT B-subunit, respectively, and pLMP3 expressing the CT A-subunit on a compatible plasmid, all from *lac* promoters, have been described

* Corresponding author. Mailing address: GI Cell Biology, Enders 720, Children's Hospital Boston, 300 Longwood Ave., Boston, MA 02115. Phone: (617) 919-2573. Fax: (617) 730-0498. E-mail: wayne.lencer@childrens.harvard.edu.

▽ Published ahead of print on 22 January 2008.

previously (12). A clone (pMGJ173) expressing both G33D and W88K variants in a single isopropyl-β-D-thiogalactopyranoside (IPTG)-inducible operon was constructed by inserting the G33D variant gene from pLMP148 as a BamHI-(BstXI made blunt using T4 DNA polymerase) fragment into BamHI-SmaI-digested pLMP133. *Escherichia coli* TE1 carrying pLMP3 was then transformed with pMGJ173. The large-scale culture conditions used for IPTG induction and purification of milligram quantities of variant holotoxins from polymyxin B-treated periplasmic extracts followed by Talon affinity column purification have been described previously (11).

Preparation of DRMs by sucrose equilibrium density centrifugation. Toxins were applied for 1 h at 4°C to apical membranes of confluent monolayers of T84 cells grown on 45-cm^2 permeable supports. Detergent-resistant membranes (DRMs) were isolated as described previously (35). Floating and soluble fractions were collected and analyzed by Western blotting.

Endocytosis of wt CT or CT W88K/G33D. For the isotopic studies, toxins were iodinated with $Na^{125}I$ using iodobeads (Pierce) and purified as described previously (15). Twenty nanomolar ^{125}I-labeled toxin was added to either the apical or basolateral surface of T84 cell monolayers (0.33 cm^2), which were then incubated for 1 h at 4°C to saturate the cell surface receptors. The monolayers were then warmed to 37°C in the presence of freshly applied 20 nM ^{125}I-labeled toxin for 10 or 30 min and then rapidly cooled to 4°C and washed extensively in ice-cold HBSS. Surface-bound toxin was then removed by immersing the monolayers in HBSS buffered to pH 2.5 using two 5-min incubations at 4°C ("acid stripping" as described by Wolf et al. [35]). The monolayers were then washed again in HBSS (pH 7.4) and cut from the plastic supports, and ^{125}I-labeled toxin uptake was analyzed by gamma counting.

For the immunoblot experiments, T84 cells grown on 5-cm^2 permeable supports were exposed apically as described above to unlabeled toxin for either 5 or 10 min at 37°C and then washed and acid stripped exactly as described above. The inserts were then excised, and the cells were lysed. The wt and chimeric toxins were immunoprecipitated from cell extracts using antibodies raised against the denatured CT B-subunit (17). Immunoprecipitates and total cell extracts were then analyzed by sodium dodecyl sulfate (SDS)-polyacrylamide gel electrophoresis (PAGE) and immunoblotting as previously described (17).

Coimmunoprecipitation of toxin and ganglioside GM_1, gel electrophoresis, and immunoblotting. Polarized cells were treated apically or basolaterally with the toxins at 4°C, washed, and then scraped into buffer containing 0.34 M sucrose, 10 mM HEPES, 1 mM EDTA, and 0.1 mM $MgCl_2$ at 4°C. Cells were then extracted in 2 ml of buffer containing 150 mM NaCl, 5 mM EDTA, 1% Triton X-100, 1.25% *n*-octyl-β-D-glucopyranoside, 0.25% SDS, and 0.1% bovine serum albumin supplemented with Complete protease inhibitor mixture (Roche Molecular Biochemicals) (24). The B-subunit of CT was immunoprecipitated overnight at 4°C using antibodies specific to the CT B-subunit coupled to polystyrene beads (Polyscience). Immune complexes were recovered by centrifugation, and coimmunoprecipitated GM_1 and toxin were released by boiling in SDS buffer. Samples were run on polyacrylamide gels and transferred to nitrocellulose. GM_1, which was at the dye front, was transferred to the membrane in the absence of methanol and detected by ligand blotting using 3 nM horseradish peroxidase (HRP)-labeled CT B-subunit (Sigma). Toxins were identified by use of polyclonal rabbit antiserum raised against the CT A- and B-subunits. The CT B-subunit antibody cross-reacted with the B-subunit of all of the mutant toxins. In some studies band densities were quantified by densitometry using a Kodak Digital Science 440 CF image station (PerkinElmer Life Sciences). All signals were in the linear range.

Fluorescent labeling of toxin and FRAP studies. wt CT B-subunit or CT W88K/G33D was labeled with monofunctional Cy3 (GE Healthcare) according to the manufacturer's instructions. Cy3-CT B-subunit (90 nM) or Cy3-chimera (200 nM) was applied to COS-7 cells at 4°C for 5 min in phenol red-free Dulbecco modified Eagle medium supplemented with 25 mM HEPES and 1 mg/ml bovine serum albumin. After unbound toxin was washed away, the cells were transferred to a microscope for fluorescence recovery after photobleaching (FRAP) analysis. FRAP experiments were carried out using a Zeiss LSM 510 confocal microscope (Thornwood, NY) as previously described (13), except that for the current measurements a 4-mm-diameter circular bleach region was utilized instead of a strip. Using this bleach geometry, the diffusion coefficient (D) could be calculated directly from the half time of recovery ($t_{1/2}$) and radius (w) of the uniformly illuminated circular region as follows: $D = 0.224w^2/t_{1/2}$ (1, 27, 31). The D values for the toxins obtained using this approach are in excellent agreement with our previous estimates of the D obtained using a different bleach region geometry and analysis method (13). Mobile fractions (Mf) were calculated as previously described (13). All FRAP measurements were carried out at 22°C.

Statistics. Data were analyzed using Statview 512+ software (Brainpower, Inc., Calabasa, CA).

RESULTS

Preparation of mutant CT holotoxins. To prepare a mixture of mutant CT holotoxins containing one, two, or no binding sites for GM_1, we cotransfected into *E. coli* two plasmids, one encoding the A-subunit and the other encoding two B-subunit monomers with single inactivating substitutions in each coding region at different sites in the GM_1 binding pocket (for either Trp88 or Gly33). This resulted in assembly of a pentameric B-subunit containing both mutant monomers (a chimeric B-subunit) or in assembly of a homopentameric B-subunit containing only one of the mutant monomers.

The homopentameric B-subunits (CTB-W88K and CTB-G33D) have inactivating mutations in all five GM_1 binding sites and thus cannot bind GM_1 at all (10). Pentamers containing a mixture of the two monomers (CTB-W88K/G33D), however, have one or two structurally intact and functional binding sites, but no more. This is because one B-subunit monomer containing a W88K substitution and the native G33 residue interacts with an adjacent B-subunit monomer containing a G33D substitution and the native W88 residue to form a functional GM_1 binding pocket identical to that in wt toxin, and all possible combinations of the two mutant monomers allow formation of only one or two functional binding pockets in the assembled pentameric B-subunit (Fig. 1A).

The G33D and W88K substitutions in the B-subunits had no apparent effect on assembly with the A-subunit to form holotoxin, as assessed by immunoprecipitation of the CT B-subunit followed by SDS-PAGE and immunoblotting for the A- and B-subunit monomers (using antibodies that recognize either the A- or B-subunits) (Fig. 1B). To show that the chimeric toxins contained B-subunit pentamers composed of both G33D and W88K monomers, we analyzed unboiled samples of the toxin mixtures under nonreducing conditions using nonreducing SDS-PAGE followed by Coomassie blue staining (Fig. 1C). Because of the change in electrical charge caused by the substitution of Asp for Gly, the mutant G33D homopentamer migrated more slowly than the mutant W88K or wt homopentamer (Fig. 1C, compare lane 6 with lanes 2 to 4). The A-subunit migrated faster than the pentameric B-subunits (lanes 3 to 5). The mixture of chimeric toxins, CT W88K/G33D, produced four major protein bands, two of which corresponded to the CTB-G33D and CTB-W88K homopentamers (Fig. 1C, lane 5). The two intermediate bands represent B-subunit pentamers containing mixtures of G33D and W88K. Thus, the two monomers assembled stably into chimeric B-subunits that associated with the A-subunit to form holotoxin.

Cross-linking of three or more ganglioside GM_1 molecules by CT is not required for toxicity but strongly enhances toxin action. We first examined the abilities of the wt CT and chimeric CT W88K/G33D toxins to induce an Isc from polarized human intestinal T84 cells. When applied to apical cell membranes, the chimeric toxins (10 nM) induced Cl^- secretion, indicating that the mutant B-subunit monomers complemented each other as predicted. The results also indicated that binding only one or two GM_1 molecules was sufficient for toxicity, consistent with previous studies of De Wolf et al. performed with chimeric holotoxins with chemically modified B-subunit polypeptides (6). The toxicity induced by chimeric CT W88K/G33D, however, was markedly attenuated com-

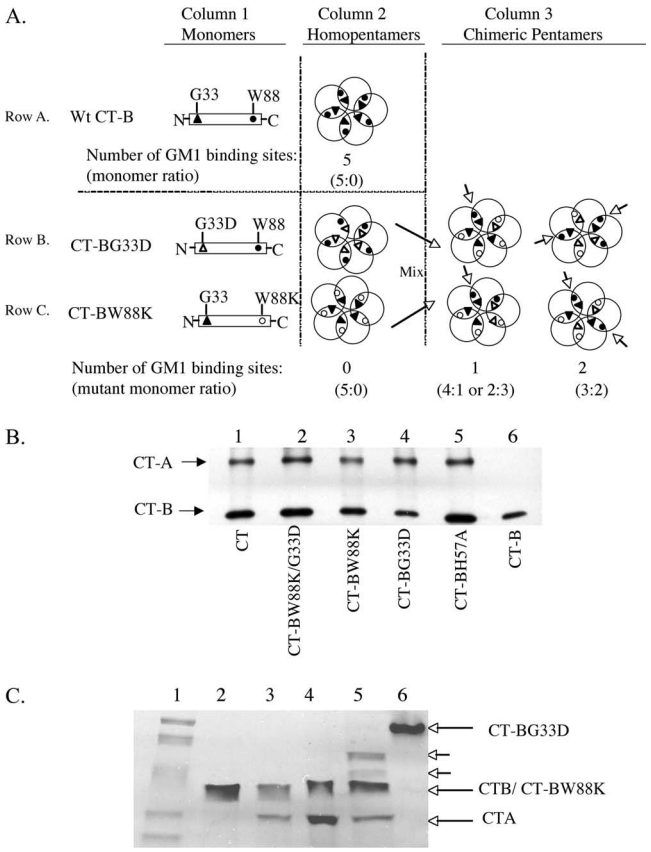

FIG. 1. Production of the mutant holotoxin containing chimeric B-subunit pentamers with CTB-W88K/G33D. (A) Schematic diagram showing B-subunit monomers (column 1) for wt CT B-subunit (row A), CTB-G33D (row B), and CTB-W88K (row C), the corresponding B-subunit homopentamers (column 2), and examples of mixed chimeric pentamers (column 3). Pentameric B-subunits are represented by five interlocking circular monomers. Amino acids G33 and W88, located in the N- and C-terminal regions of the wt CT B-subunit polypeptide, are indicated filled triangles and filled circles, respectively. The single amino acid substitutions G33D and W88K are indicated by open triangles and open circles, respectively. G33 and W88 contribute to the formation of wt binding sites for GM_1 between adjacent monomers; wt sites are indicated by the presence of both filled triangles and filled circles in the binding pockets between neighboring monomers. The wt CT B-subunit has five binding sites for GM_1 (column 2, row A), while the mutant homopentamers CTB-G33D and CTB-W88K, containing five identically substituted B-subunits, have none (column 2, rows B and C). When the CTB-W88K and CTB-G33D plasmids are coexpressed, the resultant pentameric B-subunits can be mutant homopentamers with no binding sites for GM_1 (column 2, rows B and C) or chimeric pentamers with either one or two binding sites for GM_1 (column 3, rows B and C), depending on the ratio of the individual monomers incorporated into the pentamer. Small arrows indicate binding sites for GM_1 in chimeric pentamers. (B) Mutant B-subunits, including CTB-W88K/G33D, CTB-W88K, CTB-G33D, and CT-H57A (lanes 2 to 5), assembled with the A-subunit as efficiently as wt CT B-subunit (lane 1) to form holotoxin. Toxins were immunoprecipitated by antibodies to the B-subunit, run on SDS-PAGE gels, and immunoblotted using antibodies against the CT A- and B-subunits. (C) wt and mutant toxins or B-subunit pentamers evaluated by SDS-PAGE under nonreducing conditions and without boiling of the samples. Lane 2, wt CT B-subunit; lane 3, wt CT; lane 4, CTB-W88K; lane 5, CT W88K/G33D; lane 6, CTB-G33D. Under these conditions, B-subunit pentamers do not dissociate. Lane 1 contained molecular mass markers (from the top to the bottom, 66, 45.5, 36, 29, and 24 kDa). Under these conditions the CT A-subunit disassociated from the B-subunit and ran at approximately 30 kDa. The B-subunit remained as a pentamer and migrated based on the molecular weight, as well as the charge. As indicated by the large arrows, CTB-W88K (lane 4) migrated similar to wt CT B-subunit (lanes 2 and 3), while CTB-G33D (lane 6) migrated much higher in the gel. The mixture of CT W88K/G33D toxins contained at least four structurally distinct pentamers: CTB-W88K, a small amount of CTB-G33D, and two additional pentamer forms (indicated by the small arrows) comprising combinations of CTB-G33D and CTB-W88K. The stoichiometry of the monomers making up each pentamer could not be determined by the method used.

pared to that of wt CT (Fig. 2A). The maximal Isc induced by the chimeric toxins was only 20% of the wt CT Isc (Fig. 2C, compare columns 2 and 3), and the onset of toxin-induced Cl^- secretion (a measure of toxin transport from the PM to the ER [8]) was delayed ~30% (from 43 ± 0.8 min to 58 ± 3.5 min [means ± standard deviations; $n = 14$]) (Fig. 2A and B). Holotoxins with homopentameric B-subunits consisting of mutant CTB-W88K or CTB-G33D polypeptides could not bind GM_1, and they were completely inactive, as predicted (Fig. 2A and 2C, columns 8 to 11) (10). The cAMP agonist vasoactive intestinal peptide was added at the end of the time course to induce Cl^- secretion by another cAMP-dependent mechanism in order to calibrate measurement of Isc and demonstrate monolayer viability (Fig. 2A). Nearly identical results were obtained when the toxins were applied to basolateral cell surfaces (Fig. 2B), showing that multivalent (three or more molecules) binding of GM_1 by CT affects toxin entry into the ER via both the apical and basolateral endocytic pathways. Dose-response studies demonstrated that the chimeric toxins remained strongly attenuated even at concentrations that were as much as 100-fold greater than that of wt CT (Fig. 2C, compare columns 2, 3, and 5 to 7; unpublished results).

To show that the secretory response induced by the chimeric toxins required binding to GM_1 specifically, we tested for inhibition of Isc by competition with excess wt CT B-subunit. Pretreatment of T84 cells with a 100-fold excess wt CT B-subunit strongly inhibited the Isc induced by the chimeric toxins (Fig. 2C, compare columns 3 and 4). To demonstrate that the homopentameric mutant CTB-W88K or CTB-G33D did not interfere with the functional response to the chimeric CT W88K/G33D toxins (the mutant homopentamers were also present in the chimeric toxin mixture), we tested for competitive inhibition using mutant homopentameric CTB-W88K or CTB-G33D. In contrast to the results obtained for competition with excess wt CT B-subunit, a 100-fold excess of CTB-W88K or CTB-G33D did not affect the toxicity induced by either wt CT (Fig. 2D) or the chimeric mutant CT W88K/G33D (Fig. 2E).

Thus, a mutant toxin containing only one or two binding sites for GM_1 induces toxicity in T84 cells, indicating that there is transport from the PM to ER (8). The slower onset and strong attenuation of toxin function, however, suggest that the chimeric toxins enter the ER of T84 cells with a lower efficiency than wt CT.

Toxin binding to GM_1 at the cell surface. One problem in interpreting the results of these functional studies was that the chimeric toxins, which contained only one or two native binding sites for GM_1, were also predicted to have lower avidity for

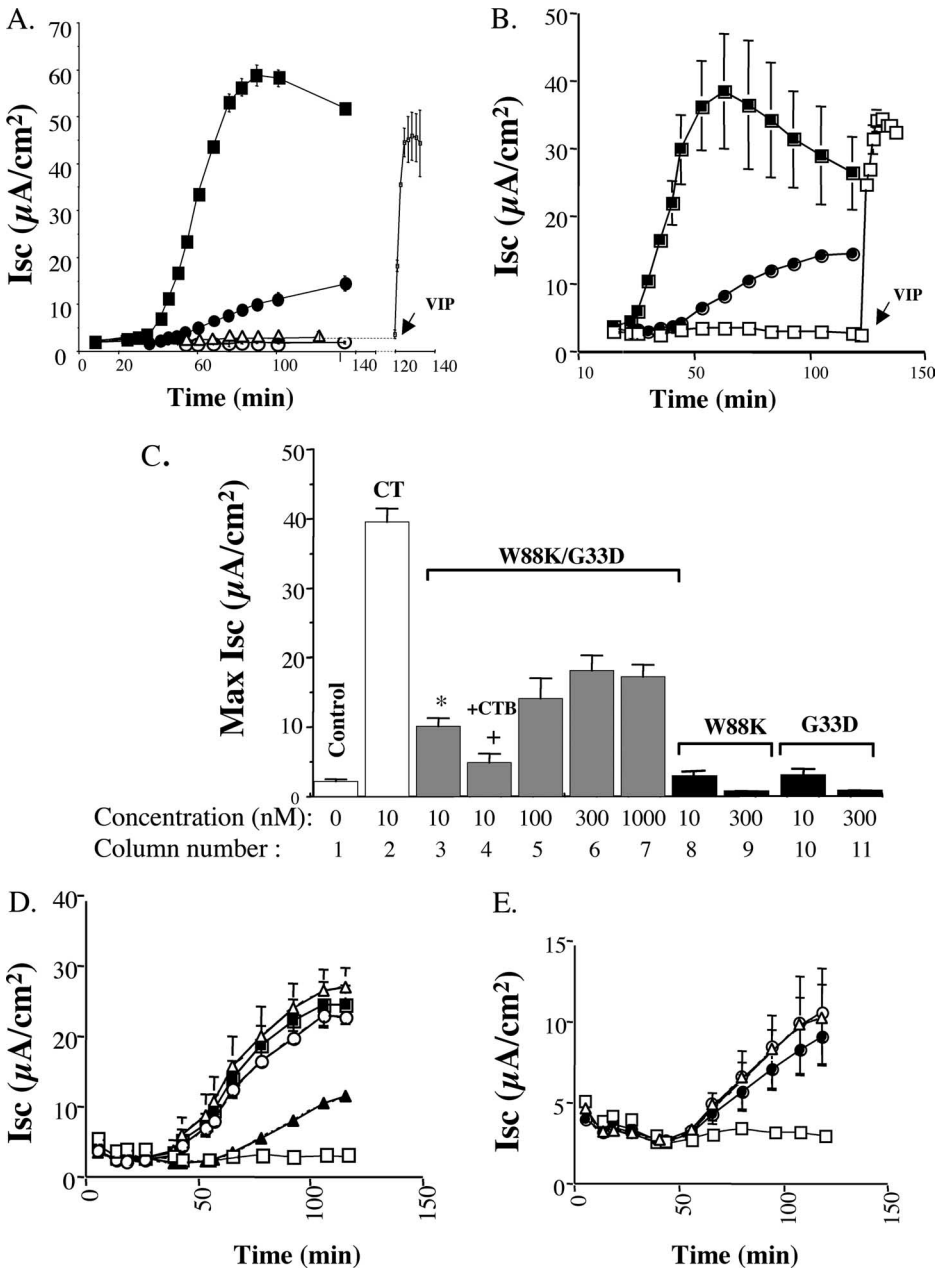

FIG. 2. Chimeric CT W88K/G33D toxin induces an attenuated chloride secretory response in T84 cells. (A) Representative time course of apical toxin-induced chloride secretion in response to treatment with 10 nM wt CT (■) or CT W88K/G33D (●) or with CTB-W88K and CTB-G33D (△ and ○, respectively). As indicated by the arrow, the cAMP agonist vasoactive intestinal peptide (VIP) was added at the end of the time course to control monolayers to demonstrate equivalency of the secretory response and monolayer viability. The error bars indicate the variance calculated as the standard deviation ($n = 2$). The data are representative of the results of eight experiments. (B) Representative time course of basolateral toxin-induced chloride secretion in response to treatment with 10 nM wt CT (■) or CT W88K/G33D (●) or in untreated controls (□). The symbols indicate the averages for two monolayers; the error bars indicate the variance calculated as the standard deviation ($n = 2$). The data are representative of the results of two experiments. (C) Bar graph summarizing data from multiple independent experiments, showing the maximal (Max) Isc induced by wt CT (column 2) ($n = 15$), 10 nM CT W88K/G33D alone (column 3) ($n = 14$) or with 1 μM wt CT B-subunit as a competitive blocker (column 4) ($n = 6$), concentrations of CT W88K/G33D ranging from 100 to 1,000 nM (columns 5 to 7) ($n = 4$ to 6), and CTB-W88K and CTB-G33D at a concentration of 10 nM (columns 8 and 10, respectively) ($n = 8$) or 300 nM (columns 9 and 11, respectively) ($n = 4$). The error bars indicate standard errors. The P value is ≤0.05 for comparisons of columns 3 and 2 (asterisk) and columns 4 and 3 (plus sign). (D) Time course demonstrating that Cl^- secretion induced by 10 nM CT (■) can be inhibited by preincubation with 1 μM CT B-subunit (▲) but not by CTB-W88K (△) or CTB-G33D (○). Control monolayers were included (□). The data are representative of the results of two experiments. (E) Time course demonstrating that Cl^- secretion induced by 10 nM CT W88K/G33D (●) is not inhibited by preincubation with CTB-W88K (△) or CTB-G33D (○). Control monolayers were included (□). In panels D and E the data are representative of the results of two experiments. The symbols indicate the means for two monolayers; the error bars indicate the variance calculated as the standard deviation ($n = 2$). μA, microamperes.

binding GM_1 than wt CT. To address this issue, we first measured binding of the wt CT and chimeric CT W88K/G33D toxins to T84 cell apical membranes.

At 4°C, increasing the concentrations of the wt and chimeric toxins resulted in similar steady-state binding to apical membranes of polarized T84 intestinal cells (Fig. 3A). However, when the wt or chimeric toxin was used to compete with the binding of a tracer wt CT B-subunit (CTB-HRP), the results revealed an almost 2-log-lower apparent affinity of the chimeric toxin to bind to T84 membranes (Fig. 3B). Thus, as predicted for a toxin with only one or two native binding pockets, the binding affinity of the chimeric toxin for GM_1 was less than that of wt CT.

Nonetheless, the chimeric toxins exhibited binding to GM_1 in T84 cell membranes that was sufficiently stable to result in coimmunoprecipitation of the bound GM_1 with toxin-antitoxin complexes (Fig. 3C). In these studies, the toxins were applied to T84 cells at 4°C to allow maximal binding at steady state. After washing, the cells were solubilized, and the CT-GM_1 complexes were immunoprecipitated using antibodies against the B-subunit. Like wt CT, the CT W88K/G33D chimeric toxins, with only one or two wt GM_1 binding pockets, remained bound to GM_1 during solubilization and immunoprecipitation. In contrast, the homopentameric CTB-W88K and CTB-G33D mutant toxins (which had inactivating mutations in all GM_1 binding pockets) did not remain bound to GM_1. Quantification of these results by densitometry showed that the CT W88K/G33D chimeric toxins immunoprecipitated about fivefold less GM_1 than wt CT, consistent with a chimeric B-subunit containing only one or two native binding pockets for GM_1.

To see if GM_1 coimmunoprecipitated with a toxin containing mutations that decreased (but did not eliminate) the binding affinity for GM_1 in all five binding pockets, we used mutant toxin CT-H57A (24). The avidity for CT-H57A binding of GM_1 on cell membranes was approximately 1.5 logs lower than that for wt CT binding, which was very similar to that found for the chimeric toxins CT W88K/G33D. In contrast to the results for CT W88K/G33D, however, we found that the CT-H57A mutant toxin did not coimmunoprecipitate with GM_1 (Fig. 3C, compare lane 6 with lanes 2 and 3). When tested for toxicity with T84 cells, the chimeric toxins were more potent than the mutant CT-H57A toxin (Fig. 3D), suggesting a direct effect on toxin function of interaction with GM_1 via native binding sites or clustering of GM_1 or both.

Evidence for toxin binding to lipid rafts. Because the toxicity of the wt AB_5 toxins correlates with the ability of GM_1 to associate with lipid rafts and because the chimeric toxins are functional (although strongly attenuated), we next tested if the CT W88K/G33D chimeric toxins retained the ability to associate with DRM fragments, the presumed biochemical correlates of lipid rafts (20, 28). We found that the CT W88K/G33D chimeric toxins retained the ability to fractionate with DRMs, although the proportion of bound chimeric toxin in the DRM-associated fraction appeared to be somewhat less than the proportion of wt CT (Fig. 4A). All of the homopentameric mutant CTB-W88K, which bound T84 cell membranes most poorly, was found in the soluble fractions. Thus, binding to only one or two GM_1 molecules in cell membranes was suffi-

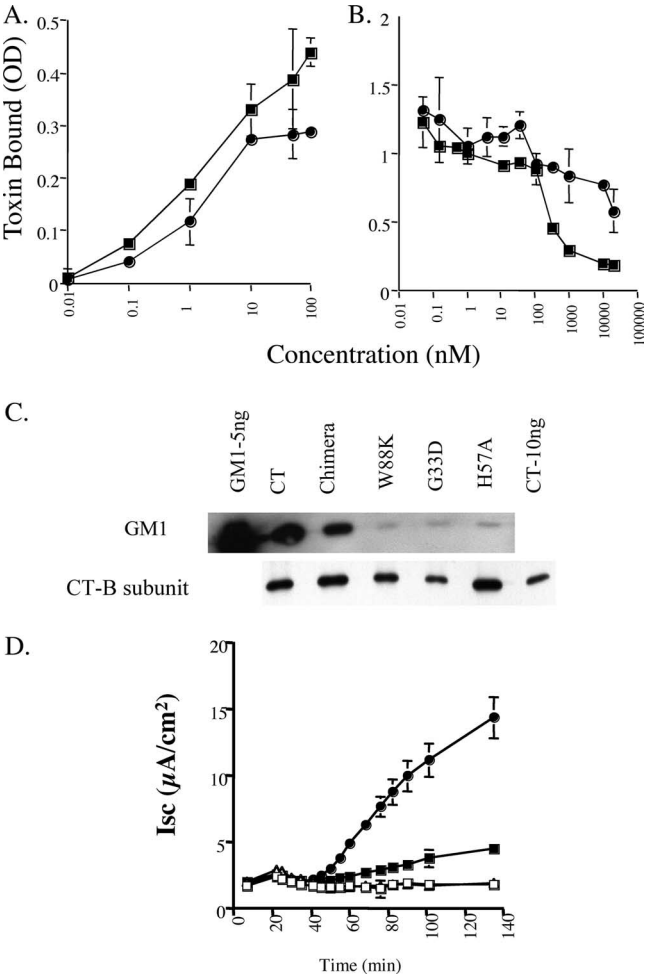

FIG. 3. Chimeric CT W88K/G33D toxins display unique biology as assessed by binding of GM_1 and induction of toxicity. (A) Representative steady-state binding of wt CT B-subunit (■) and CT W88K/G33D (●) to the cell surface membranes of T84 cells at 4°C as determined by a modified enzyme-linked immunosorbent assay. The optical density (OD) was a direct measure of the amount of the bound toxin in this assay system. The data are the means ± standard deviations for three monolayers and are representative of the results of three independent experiments. (B) Representative curve showing binding of 3 nM HRP-labeled CT B-subunit competing with different concentrations of wt CT B-subunit (■) or CT W88K/G33D (●) on the surface of T84 cells at 4°C. The data are the means ± standard deviations for three monolayers. For some concentrations the standard deviation is obscured by the symbol. The data are representative of the results of two independent experiments. (C) Immunoprecipitation of toxin B-subunits and coimmunoprecipitation of GM_1 from extracts of T84 cells preincubated with toxins at 4°C and washed before extraction. The left and right lanes contained purified GM_1 (5 ng) and CT (10 ng), respectively, as controls. The other lanes (from left to right) contained extracts from cells preincubated with wt holotoxin (CT), CT G33D/W88K (chimera), or a homopentameric mutant (CTB-W88K, CTB-G33D, or CT-H57A). Toxin B-subunits were detected by immunoblotting (lower panel), and GM_1 was detected using HRP-labeled CT B-subunit as a ligand blot (upper panel). The data are representative of the results of two independent experiments. (D) Representative toxin-induced chloride secretory response to 10 nM CT-H57A (■), CT W88K/G33D (●), CTB-W88K (△), or CTB-G33D (□) (CTB-W88K and CTB-G33D data are superimposed). The data are representative of the results of three experiments. The error bars indicate the variance calculated as the standard deviation ($n = 2$). μA, microamperes.

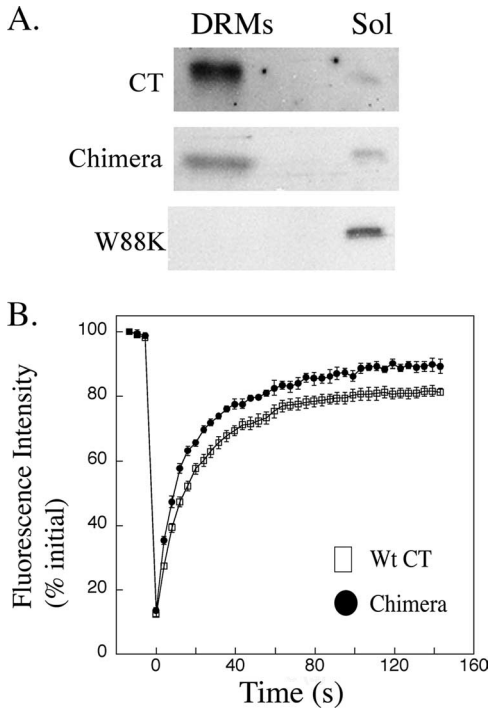

FIG. 4. Both wt CT and the CT W88K/G33D chimeric toxins associate with DRMs and display low lateral mobility in PM consistent with localization to lipid raft microdomains. (A) Immunoblots for wt CT B-subunit (upper panel), CT W88K/G33D chimera (middle panel), and CTB-W88K (lower panel), showing association of toxins with DRM or soluble (Sol) fractions isolated from T84 cells preincubated with the indicated toxins at 4°C. The data are representative of the results of two independent experiments. (B) Representative FRAP curves for wt CT and mutant CT W88K/G33D FRAP measurements in COS-7 cells. COS-7 cells were incubated with Cy3-CT B-subunit (Wt CT) or Cy3-chimera (Chimera) and subjected to confocal FRAP using a 4-mm-diameter circular bleach region at time zero. Fluorescence recovery in the bleach region was recorded over time and normalized to the prebleach intensity. The data are representative of the results of five experiments and are the means ± standard errors for FRAP measurements for 7 to 10 individual cells.

cient for the chimeric toxins to associate with DRMs, consistent with results of studies of GM_1 itself (23).

We next used FRAP to determine the membrane *D* values for wt and CT W88K/G33D chimeric toxins bound to living COS-7 cells, which display high levels of wt CT binding (13, 21). FRAP measures the lateral mobility of proteins in membranes in real time (i.e., *D* and Mf) and thus can assess the degree to which the movement of toxin-GM_1 complexes in the plane of the membrane is constrained. A previous FRAP analysis showed that the diffusional mobility of CT in COS-7 cells is unusually low compared to that of other lipid-anchored raft proteins, which suggested that the toxin is localized to lipid rafts (13).

Fluorophore-labeled wt and chimeric mutant toxins were incubated with COS-7 cells at 37°C for 5 min, washed extensively to remove unbound toxin, and studied by performing a confocal FRAP analysis as described in Materials and Methods. Under these conditions, the CT W88K/G33D toxins had low lateral *D* values and high Mf values, similar to the results obtained for wt CT (Fig. 4B and Table 1). Thus, both the wt and chimeric toxins were constrained from free diffusion in the PM, consistent with binding to GM_1 localized within membrane microdomains. We also noted small but statistically significant increases in both *D* and Mf for the chimera toxins compared to the wt CT B-subunit. Because the fraction of CT B-subunit internalized by endocytosis contributes to the immobile fraction (immobile fraction = 1 − Mf) (13), the increase in Mf could reflect a lower rate of endocytosis for the chimeric toxins; and the increase in *D* might reflect slightly less efficient tethering to membrane microdomains by the chimeric toxin, consistent with our GM_1 binding results.

Endocytosis. Finally, to investigate further why the CT W88K/G33D chimeric toxins are less potent, we examined their ability to enter the T84 monolayers by endocytosis. For these experiments, T84 monolayers were incubated with either 10 nM unlabeled toxin or 20 nM ^{125}I-labeled toxin at 37°C for 5, 10, or 30 min and then cooled to 4°C. After cell surface-bound toxins were removed by acid stripping (see Materials and Methods), the mass of toxin internalized by endocytosis was measured either by SDS-PAGE and immunoblotting of total cell lysates using antibodies against the B-subunit monomer (Fig. 5A) or by gamma counting (Fig. 5B and C). These studies showed that after 5 and 10 min of uptake, a greater mass of wt CT than of the chimeric toxins entered the cells. After 30 min of incubation, the mass of chimeric toxins taken up approached the mass of the wt toxin taken up. Similar results were obtained for entry of the toxins via the basolateral membrane (Fig. 5C). Thus, both wt CT and CT W88K/G33D chimeric toxins enter T84 cells by endocytosis, but the wt CT, which can bind five GM_1 molecules simultaneously, is internalized more efficiently.

DISCUSSION

Our studies show that binding of chimeric CT to GM_1 via only one or two native GM_1 binding sites is sufficient for both the association with lipid rafts and the induction of toxicity, thus indicating that the chimeric toxins reach the ER to allow for retrotranslocation of the A1 chain to the cytosol. The result also suggests the presence of an endogenous pathway for GM_1 to enter the ER from the cell surface. Binding to only one or two GM_1 molecules, however, attenuates the toxicity of the chimeric toxins, consistent with the results of a previous study performed with chimeric CTs containing mixtures of chemically modified CT B-subunit polypeptides (6). The lower toxicity observed for the chimeric toxins is associated with both a lower rate of toxin endocytosis and a slower time course of toxin action. Thus, the stoichiometry of binding to GM_1 by the CT B-subunit appears to play a rate-limiting role in toxin entry and trafficking, presumably by affecting the efficiency of endo-

TABLE 1. Diffusional mobility of wt and chimeric CT B-subunit measured by confocal FRAP (temperature, 22°C)[a]

Protein	*D* ($\mu m^2/s$)	% Mobile	*n*
Cy3-CT B-subunit	0.058 ± 0.018	76.9 ± 1.0	42
Cy3-chimera	0.068 ± 0.018	82.5 ± 1.2	40

[a] The values are means ± standard errors based on pooled data from five independent experiments.

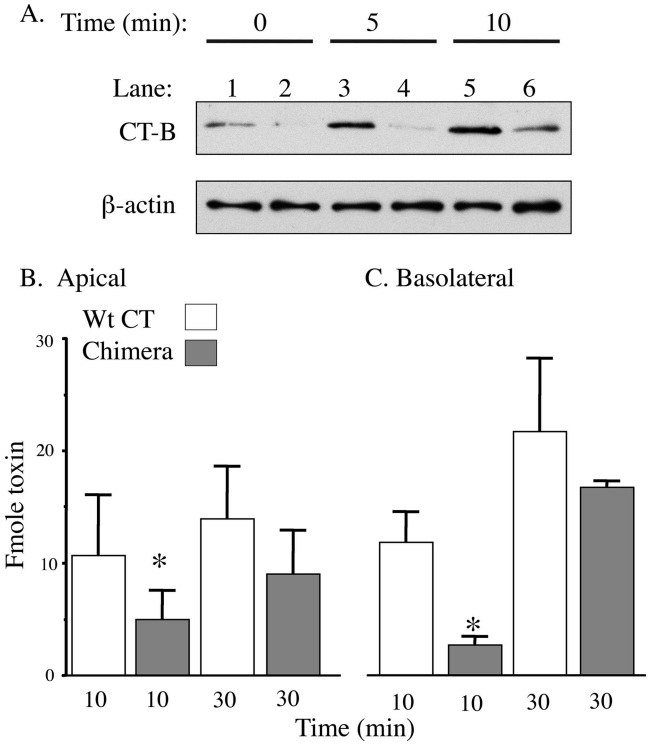

FIG. 5. CT W88K/G33D is endocytosed less efficiently that wt CT. (A) Immunoblots of extracts from cells allowed to endocytose toxins. T84 monolayers were treated with 10 nM wt CT (lanes 1, 3, and 5) or CT W88K/G33D (lanes 2, 4, and 6) at 4°C for 1 h and then incubated with the same toxin at 37°C for 0 (control for surface binding), 5, or 10 min, as indicated. Cells were then cooled to 4°C, washed, and acid stripped. Toxins were immunoprecipitated from total cell lysates as described in Materials and Methods. The upper panel shows the mass of toxin internalized by endocytosis as measured by SDS-PAGE and immunoblotting using antibodies against the B-subunit monomer. The lower panel is a blot of the same cell extracts for β-actin as a loading control. Comparisons of lane 3 with lane 4 and of lane 5 with lane 6 showed that more wt CT than CT W88K/G33D was endocytosed at 5 and 10 min. Typically, between 3 and 8% of apical membrane-bound wt toxin is internalized by 10 min at 37°C (26). (B and C) Bar graphs summarizing receptor-mediated endocytosis of 20 nM ^{125}I-labeled CT (open bars) and ^{125}I-labeled chimeric CT W88K/G33D (shaded bars) at 10 and 30 min from either the apical (B) or basolateral (C) surface of polarized intestinal T84 cells. Significantly more wt CT than chimeric CT was endocytosed from both the apical and basolateral cell surfaces at 10 min. The bars indicate the means, and the error bars indicate the standard errors ($n = 5$ for the apical surface; $n = 2$ to 5 for the basolateral surface). Asterisk, $P \leq 0.05$ for a comparison of early and late time points.

cytosis and GM_1-dependent sorting during retrograde trafficking through the secretory pathway.

We sought to control for the effect of binding avidity on toxin action in these studies by using the mutant toxins CT-H57A, CTB-G33D, and CTB-W88K. Each of these toxins has a homopentameric B-subunit containing five identical binding sites for GM_1. In the case of CTB-G33D and CTB-W88K, the B-subunits cannot bind or bind very poorly to GM_1, and they are inactive, as described previously (10). The CT-H57A mutant also has five identical binding pockets, but they are still functional, although attenuated for binding to GM_1. This is because the H57A mutation causes inward displacement of the Glu51-Ile58 loop that alters the interaction between the CT B-subunit and GM_1. The H57A mutation results in a toxin that can still bind GM_1, but with lower apparent affinity and less stability (24). Empirically, the steady-state GM_1 binding properties of the CT-H57A mutant and CT W88K/G33D chimeric toxins are very similar, but for different reasons.

Unlike the CT-H57A mutant, the CT W88K/G33D chimeric toxins are predicted to have one or two completely normal binding pockets for GM_1 and three or four binding pockets with no activity. This was demonstrated experimentally by the ability of the CT W88K/G33D chimeric toxin to coimmunoprecipitate with GM_1 with approximately 1:1 stoichiometry instead of the 1:5 stoichiometry observed for wt CT and by the ability of the chimeric toxins to associate stably with GM_1 in diffusion-restricted membrane regions of live cells. The CT-H57A mutant, in contrast, does not stably bind to GM_1, as assessed biochemically and by coimmunoprecipitation (24), and it is less toxic than the chimeric CT W88K/G33D toxins. Thus, the CT-H57A and CT W88K/G33D mutant toxins have different phenotypes, even though they have very similar binding affinities for GM_1 in cell membranes. These results indicate that the greater toxicity of the CT W88K/G33D variant than of the CT-H57A variant is due to the presence of one or two native GM_1 binding sites in the CT W88K/G33D chimeric toxin rather than the five lower-affinity GM_1 binding sites in the CT-H57A variant. In addition, a likely explanation for the lower capacity of the CT W88K/G33D chimeric toxin than of wt CT to induce Cl^- secretion is its inability to cross-link more than two GM_1 molecules. Because the chimeric CT W88K/G33D toxins are functional, however, the ability of wt CT to cross-link five GM_1 molecules cannot be an absolute requirement for GM_1 to mediate membrane trafficking through the retrograde pathway.

The observation that cross-linking GM_1 appears to enhance CT function might be explained by the proposed structure and function of lipid rafts in cellular physiology. So far, the bulk of the experimental data on trafficking CT in the retrograde pathway from the PM to the ER, including the results of the current study, indicate that association of the CT-GM_1 complex with lipid rafts is essential. Other proteins and lipids require clustering to associate with lipid rafts, and in some cases this is necessary for function (5, 7, 30). When measured in live cells, lipid rafts have been found to be very small (~40 to 50Å), and they are unstable and have very short half-lives (for reviews, see references 19 and 29). It has been proposed previously that cross-linking of lipid raft components may affect lipid raft function by stabilizing the lipid raft domain and/or inducing the aggregation of many small rafts (2, 9, 19, 33). The hypothesis that such cross-linking of GM_1 by the pentavalent B-subunit might affect lipid raft structure and function in T84 cells is consistent both with the results of studies of giant unilamellar vesicles, where binding by CT causes a dynamic redistribution and domain formation of L_o phase lipids (3), and with the results of the current study. Thus, although the chimeric toxins appear to associate with lipid rafts, as assessed biochemically and biophysically, it is possible that they cannot cross-link GM_1 in a way that fully stabilizes or clusters lipid rafts so as to induce or maintain optimal retrograde transport all the way from the PM to the ER.

It is also possible that cross-linking of GM_1 by CT is required

to induce membrane curvature and domain formation in a way that facilitates uptake from the PM, as recently reported for Shiga toxin that cross-links the related glycolipid GB3 (25). Presumably, the chimeric toxins that cannot cross-link more than two gangliosides would fail to do this. Even so, our results show that such high-density cross-linking is dispensable for CT function.

Based on the available data, we propose that the pentameric structure of CT and the related AB_5 toxins might have evolved because stable binding of toxin to lipid receptors in host cell membranes might induce or stabilize the function of lipid rafts or glycolipids themselves (25) as membrane trafficking platforms. The diameter of the CT B-subunit (60 Å) is similar to the diameter of lipid rafts measured in vivo (50Å) (34). As such, the B-subunit may bind as many as five GM_1 molecules in a single raft microdomain, and this may stabilize the lipid raft (or GM_1 platform) so that it can traffic more efficiently in the retrograde pathway. Alternatively, the B-subunit may cross-link and condense multiple lipid rafts into larger platforms that have an induced function. The present study demonstrated that chimeric toxins with only one or two wt ganglioside binding sites are attenuated but retain significant toxicity, suggesting an endogenous pathway for trafficking by the gangliosides and related ceramide-based glycolipids. Additional studies are needed to show unequivocally whether chimeric toxins with only one ganglioside GM_1 binding site exhibit any toxicity and to demonstrate the mechanisms by which cross-linking of ganglioside GM_1 in lipid rafts may modulate membrane dynamics, the efficiency of endocytosis, or sorting retrogradely in the secretory pathway.

ACKNOWLEDGMENTS

We thank Eric Barclay and Ryan Callery for technical assistance and Minchul Kang for assistance with the FRAP analysis.

This work was supported by National Institutes of Health grants DK48106 and DK53056 and Harvard Digestive Disease Center grant DK34854 to W.I.L., by National Institutes of Health Mentored Clinician Scientist award K08 and a research scholar award from the American Gastroenterological Association to A.A.W., and by National Institutes of Health grant AI31940 to R.K.H. A.K.K. was supported by the New Faculty Development Fund.

REFERENCES

1. **Adams, C. L., Y. T. Chen, S. J. Smith, and W. J. Nelson.** 1998. Mechanisms of epithelial cell-cell adhesion and cell compaction revealed by high-resolution tracking of E-cadherin-green fluorescent protein. J. Cell Biol. **142:**1105–1119.
2. **Anderson, R. G., and K. Jacobson.** 2002. A role for lipid shells in targeting proteins to caveolae, rafts, and other lipid domains. Science **296:**1821–1825.
3. **Bacia, K., P. Schwille, and T. Kurzchalia.** 2005. Sterol structure determines the separation of phases and the curvature of the liquid-ordered phase in model membranes. Proc. Natl. Acad. Sci. USA **102:**3272–3277.
4. **Brown, D. A., and E. London.** 2000. Structure and function of sphingolipid- and cholesterol-rich membrane rafts. J. Biol. Chem. **275:**17221–17224.
5. **Cherukuri, A., T. Shoham, H. W. Sohn, S. Levy, S. Brooks, R. Carter, and S. K. Pierce.** 2004. The tetraspanin CD81 is necessary for partitioning of coligated CD19/CD21-B cell antigen receptor complexes into signaling-active lipid rafts. J. Immunol. **172:**370–380.
6. **De Wolf, M. J., E. Dams, and W. S. Dierick.** 1994. Interaction of a cholera toxin derivative containing a reduced number of receptor binding sites with intact cells in culture. Biochim. Biophys. Acta **1223:**296–305.
7. **Fragoso, R., D. Ren, X. Zhang, M. W. Su, S. J. Burakoff, and Y. J. Jin.** 2003. Lipid raft distribution of CD4 depends on its palmitoylation and association with Lck, and evidence for CD4-induced lipid raft aggregation as an additional mechanism to enhance CD3 signaling. J. Immunol. **170:**913–921.
8. **Fujinaga, Y., A. A. Wolf, C. Rodighiero, H. Wheeler, B. Tsai, L. Allen, M. G. Jobling, T. Rapoport, R. K. Holmes, and W. I. Lencer.** 2003. Gangliosides that associate with lipid rafts mediate transport of cholera and related toxins from the plasma membrane to endoplasmic reticulum. Mol. Biol. Cell **14:**4783–4793.
9. **Harder, T., P. Scheiffele, P. Verkade, and K. Simons.** 1998. Lipid domain structure of the plasma membrane revealed by patching of membrane components. J. Cell Biol. **141:**929–942.
10. **Jobling, M. G., and R. K. Holmes.** 1991. Analysis of structure and function of the B subunit of cholera toxin by the use of site-directed mutagenesis. Mol. Microbiol. **5:**1755–1767.
11. **Jobling, M. G., and R. K. Holmes.** 2001. Biological and biochemical characterization of variant A subunits of cholera toxin constructed by site-directed mutagenesis. J. Bacteriol. **183:**4024–4032.
12. **Jobling, M. G., L. M. Palmer, J. L. Erbe, and R. K. Holmes.** 1997. Construction and characterization of versatile cloning vectors for efficient delivery of native foreign proteins to the periplasm of Escherichia coli. Plasmid **38:**158–173.
13. **Kenworthy, A. K., B. J. Nichols, C. L. Remmert, G. M. Hendrix, M. Kumar, J. Zimmerberg, and J. Lippincott-Schwartz.** 2004. Dynamics of putative raft-associated proteins at the cell surface. J. Cell Biol. **165:**735–746.
14. **Kenworthy, A. K., N. Petranova, and M. Edidin.** 2000. High-resolution FRET microscopy of cholera toxin B-subunit and GPI-anchored proteins in cell plasma membranes. Mol. Biol. Cell **11:**1645–1655.
15. **Lencer, W. I., S. H. Chu, and W. A. Walker.** 1987. Differential binding kinetics of cholera toxin to intestinal microvillus membrane during development. Infect. Immun. **55:**3126–3130.
16. **Lencer, W. I., C. Delp, M. R. Neutra, and J. L. Madara.** 1992. Mechanism of cholera toxin action on a polarized human intestinal epithelial cell line: role of vesicular traffic. J. Cell Biol. **117:**1197–1209.
17. **Lencer, W. I., S. Moe, P. A. Rufo, and J. L. Madara.** 1995. Transcytosis of cholera toxin subunits across model human intestinal epithelia. Proc. Natl. Acad. Sci. USA **92:**10094–10098.
18. **Lencer, W. I., and B. Tsai.** 2003. The intracellular voyage of cholera toxin: going retro. Trends Biochem. Sci. **28:**639–645.
19. **Mayor, S., and M. Rao.** 2004. Rafts: scale-dependent, active lipid organization at the cell surface. Traffic **5:**231–240.
20. **Munro, S.** 2003. Lipid rafts: elusive or illusive? Cell **115:**377–388.
21. **Nichols, B. J.** 2003. GM1-containing lipid rafts are depleted within clathrin-coated pits. Curr. Biol. **13:**686–690.
22. **Pacuszka, Y., R. M. Bradley, and P. H. Fishman.** 1991. Neoglycolipid analogues of ganglioside GM1 as functional receptors of cholera toxin. Biochemistry **30:**2563–2570.
23. **Panasiewicz, M., H. Domek, G. Hoser, M. Kawalec, and T. Pacuszka.** 2003. Structure of the ceramide moiety of GM1 ganglioside determines its occurrence in different detergent-resistant membrane domains in HL-60 cells. Biochemistry **42:**6608–6619.
24. **Rodighiero, C., Y. Fujinaga, T. R. Hirst, and W. I. Lencer.** 2001. A cholera toxin B-subunit variant that binds ganglioside G(M1) but fails to induce toxicity. J. Biol. Chem. **276:**36939–36945.
25. **Romer, W., L. Berland, V. Chambon, K. Gaus, B. Windschiegl, D. Tenza, M. R. Aly, V. Fraisier, J. C. Florent, D. Perrais, C. Lamaze, G. Raposo, C. Steinem, P. Sens, P. Bassereau, and L. Johannes.** 2007. Shiga toxin induces tubular membrane invaginations for its uptake into cells. Nature **450:**670–675.
26. **Saslowsky, D. E., and W. I. Lencer.** 2008. Conversion of apical plasma membrane sphingomyelin to ceramide attenuates the intoxication of host cells by cholera toxin. Cell. Microbiol. **10:**67–80.
27. **Schmidt, K., and B. J. Nichols.** 2004. A barrier to lateral diffusion in the cleavage furrow of dividing mammalian cells. Curr. Biol. **14:**1002–1006.
28. **Sharma, P., S. Sabharanjak, and S. Mayor.** 2002. Endocytosis of lipid rafts: an identity crisis. Semin. Cell Dev. Biol. **13:**205–214.
29. **Sharma, P., R. Varma, R. C. Sarasij, Ira, K. Gousset, G. Krishnamoorthy, M. Rao, and S. Mayor.** 2004. Nanoscale organization of multiple GPI-anchored proteins in living cell membranes. Cell **116:**577–589.
30. **Shogomori, H., A. T. Hammond, A. G. Ostermeyer-Fay, D. J. Barr, G. W. Feigenson, E. London, and D. A. Brown.** 2005. Palmitoylation and intracellular domain interactions both contribute to raft targeting of linker for activation of T cells. J. Biol. Chem. **280:**18931–18942.
31. **Soumpasis, D. M.** 1983. Theoretical analysis of fluorescence photobleaching recovery experiments. Biophys. J. **41:**95–97.
32. **Spangler, B. D.** 1992. Structure and function of cholera toxin and the related *Escherichia coli* heat-labile enterotoxin. Microbiol. Rev. **56:**622–647.
33. **Subczynski, W. K., and A. Kusumi.** 2003. Dynamics of raft molecules in the

cell and artificial membranes: approaches by pulse EPR spin labeling and single molecule optical microscopy. Biochim. Biophys. Acta **1610:**231–243.
34. **Varma, R., and S. Mayor.** 1998. GPI-anchored proteins are organized in submicron domains at the cell surface. Nature **394:**798–801.
35. **Wolf, A. A., Y. Fujinaga, and W. I. Lencer.** 2002. Uncoupling of the cholera toxin-G(M1) ganglioside receptor complex from endocytosis, retrograde Golgi trafficking, and downstream signal transduction by depletion of membrane cholesterol. J. Biol. Chem. **277:**16249–16256.
36. **Wolf, A. A., M. G. Jobling, S. Wimer-Mackin, M. Ferguson-Maltzman, J. L. Madara, R. K. Holmes, and W. I. Lencer.** 1998. Ganglioside structure dictates signal transduction by cholera toxin and association with caveolae-like membrane domains in polarized epithelia. J. Cell Biol. **141:**917–927.

Editor: S. R. Blanke